PERGAMON

Computers and Structures 77 (2000) 711–724

Computers & Structures

www.elsevier.com/locate/compstruc

Free vibrational analysis of axially loaded bending-torsion coupled beams: a dynamic finite element

S. Mohammad Hashemi, Marc J. Richard *

Department of Mechanical Engineering, Laval University, Québec, Que., Canada G1K 7P4

Received 21 January 1999; accepted 30 November 1999

Abstract

In this article, a dynamic finite element formulation for the free vibration analysis of axially loaded bending-torsion coupled beams is presented. Based on the Euler–Bernoulli and St. Venant beam theories, the exact solutions of the differential equations governing the uncoupled vibrations of an axially loaded uniform beam are found. Then, employing these solutions as basis functions, the analytical expressions for uncoupled bending and torsional dynamic shape functions are derived. Exploiting the principle of virtual work, together with the variable approximations based on the resulting shape functions, leads to a single frequency dependent element matrix which has both mass and stiffness properties. The application of the theory is demonstrated by an illustrative example of a bending-torsion coupled beam with cantilever end conditions, for which the influence of axial force on the natural frequencies is studied. The correctness of the theory is confirmed by the published results and numerical checks.

Keywords: Vibrations; Coupled beam; Bending-torsion; Axial load; Dynamic finite element

1. Introduction

Helicopter, propeller and also compressor and turbine blades of a high aspect ratio, all qualify (at least for their first few vibration modes) as axially loaded beams which usually have non-coincident elastic and inertial axes [1]. Applications of such elements also include the aeroelastic calculations for which coupled bending-torsional frequencies and modes are essential requirements [2–4]. Moreover, some complete plane and space frames can be represented with a reasonable accuracy as assemblages of axially loaded coupled beams connected together (some beam cross-sections representing bending-torsional coupling are shown in Fig. 1). Naturally, it is very important to take into account the coupling effects in vibration and response calculations of this type of structures. The effect of an important parameter, namely the axial force, which is usually negligible or non-existent for some structures such as aircraft wings (but not so for helicopter, turbine or propeller blades), have also to be taken into account.

The derivation of the equations of motion for the coupled bending-torsion vibrations of axially loaded beams, are studied by different authors (see e.g., Refs. [5,6]) and numerous approaches for calculating the free vibration natural frequencies and mode shapes have been proposed. The classical finite element method (FEM) [7], where beam element matrices are evaluated from the assumed fixed shape functions (such as polynomials), has been used by some investigators. A generalized linear eigenvalue problem then results. The dynamic stiffness matrix (DSM) method [8] offers a better alternative, particularly when higher frequencies and better accuracies of results are required. The stiffness

* Corresponding author. Tel.: +418-656-2190/+418-656-2199; fax: +418-656-7415.
E-mail address: mrichard@gmc.ulaval.ca (M.J. Richard).

0045-7949/00/$ - see front matter
PII: S0045-7949(00)00012-2

Nomenclature

D_f	denominator in the expressions of N_{1f}, N_{2f}, N_{3f} and N_{4f} (flexural shape functions)
D_t	denominator in the expressions of N_{1t} and N_{2t} (torsional shape functions)
$\Delta = D_f * D_t$	denominator in $[K_{DS}]^k$
$H_f = EI$	Flexural rigidity
$H_t = GJ$	Torsional rigidity
$[K_{DS}]$	overall dynamic stiffness matrix
$[K_{DS}^{\Delta}]$	upper triangular matrix obtained from K_{DS}
$[K_{DS}]^k$	DFE element stiffness matrix
$[K_{DS}]^k_{uncoupl}$	first part of $[K_{DS}]^k$ corresponding to the uniform beam element k
$[K_{DS}]^k_{coupl}$	the coupling part of $[K_{DS}]^k$
$(K_C)^k_{ij}$	components of $[K_{DS}]^k_{coupl}$; $i = 1, 2;\ j = 1, 2, 3, 4$
L	total length of the beam
NE	total number of elements
P	axial force (constant per element)
$\mathscr{W}$	total virtual work
$\mathscr{W}_{INT}$	internal virtual work
$\mathscr{W}_{EXT}$	external virtual work
$\mathscr{W}^k$	discretized virtual work due to kth element
$\mathscr{W}^k_f$	the bending part of W^k
$\mathscr{W}^k_t$	the torsion part of W^k
l_k	the length of element k
$m = \rho A$	mass per unit length
w	flexural displacement
W	amplitude of the flexural displacement
δW	test function due to the bending
ψ	torsional rotation
Ψ	amplitude of the torsional rotation ($\Psi \equiv$ Psi)
$\delta\Psi$	test function due to the torsion
x_α	distance between the mass and the elastic axes
$\xi = s/l_k$	element local coordinate, $0 \leqslant \xi \leqslant 1$
ω	rotary frequency ($\omega \equiv$ omega)

matrix, in this method, is obtained by directly solving the governing differential equation and hence all assumptions, being within the limits of the differential equations only, are less severe. This is the reason why results obtained using a DSM are often justifiably called "exact" [8]. But, the DSM formulation implies mathematical procedures which are sometimes difficult to deal with, and/or are often limited to special cases.

Here, a new dynamic finite element (DFE) is developed, which produces accurate solutions for coupled bending-torsional vibration of axially loaded beams and assemblies composed of such beams. The DFE approach extends the existing 'exact' DSM method, and can be advantageously elaborated to handle more complex cases for which the exact DSM does not exist. In other words, this method can be presented as an intermediate approach between the general 'weighted residual method' (i.e., the basis of the classical FEM) and the very interesting features of the frequency-

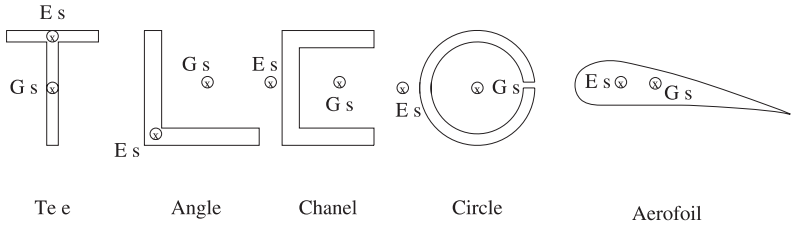

Fig. 1. Sample of beam cross-sections with non-coincident shear centre, and mass centre: E_s shear centre, G_s mass centre.

dependent exact DSM formulation. Similarly to the DSM method, the method is an efficient tool for handling the periodical structures, or systems composed of several identical substructures, having the same dynamic stiffness components and frequency characteristics. In addition, the resulting eigenvalue problem is also a non-linear one. Application of the developed methodology includes coupled bending-torsional frequency and mode calculations of rotating beam-like structures such as helicopter, propeller, turbine and compressor blades, etc. In this case, the stiffening effect due to the axial centrifugal force, cause some considerable modifications in the natural frequencies and modes, which have to be accounted for in the dynamic analysis of rotating structures. In the real blade designs, the three degrees of freedom of the rotating blades, namely flap, lag and torsion, are usually treated together in what is termed coupled mode methods [9]. Here, we investigate the coupled out-of-plane (flapping) bending-torsion free vibrations of a uniform beam element of symmetric cross-section, in the presence of a constant axial load. However, the effects of variable centrifugal force, geometrical parameters and mechanical properties, could also be introduced in the formulation by similar manners as presented in the previous works of the authors dealing with the vibrational analysis of non-uniform beams [10], the rotating of uniform and tapered beams [11–13], and the free vibration of bending-torsion coupled beams [14,15].

The differential equations, governing the uncoupled bending and torsional vibrations of an axially loaded uniform beam element, are solved in an exact sense. Then, the resulting solutions are used as basis functions and lead to the dynamic shape functions, which are exploited to derive the corresponding stiffness matrix. The method of incorporating the derived stiffness expressions in a computer program for the vibration analysis of axially loaded beams, having a non-coincident shear centre and mass centre, is discussed with some reference to an established algorithm [16,17]. The application of the theory, in the absence of the axial force, is demonstrated by an illustrative example of cantilever beam, wherein a substantial amount of coupling between the bending and torsion are highlighted. Thereafter, the influence of the axial force on the coupled bending-torsional frequencies is investigated.

2. Mathematical model

Consider a uniform beam element of length L with the mass axis and the elastic axis (which are respectively the loci of the mass centre and the shear centre of the cross-sections) being separated by a distance x_α. In the right-handed coordinate system of Fig. 2, the elastic axis which is assumed to be coincident with the y axis is a permitted flexural translation $w(y,t)$ in the z direction and a torsional rotation $\psi(y,t)$ about y axis, where y and t denote the distance from the origin and time, respectively. A constant axial load P is assumed to act through the centroid (mass centre) of the cross-section. P is considered to be positive when in traction.

Using the coupled Bernoulli–St. Venant bending-torsion beam theory (i.e., neglecting shear deformation, rotary inertia and warping of the cross-section), the governing partial differential equations of motion of the beam shown in Fig. 2, are given by [18]

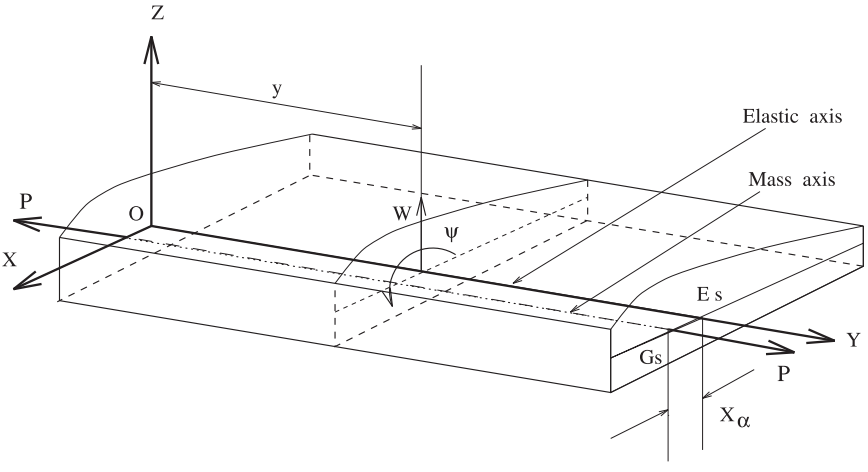

Fig. 2. Coordinate system and notations for coupled bending-torsional vibration of a uniform beam element: E_s shear centre, G_s mass centre.

$$H_f w'''' - P w'' + m\ddot{w} + (P x_\alpha \psi'' - m x_\alpha \ddot{\psi}) = 0, \tag{1}$$

$$(H_t + P(I_\alpha/m))\psi'' - I_\alpha \ddot{\psi} - (P x_\alpha w'' - m x_\alpha \ddot{w}) = 0 \tag{2}$$

with appropriate boundary conditions imposed at $y = 0, L$. For example,

clamped: $y = 0, \quad w = w' = \psi = 0,$

free: $y = L, \quad w'' = w''' = \psi' = 0,$ etc.

H_f and H_t are, respectively, the bending and torsional rigidity of the beam; m is the mass per unit length; I_α is the polar mass moment of inertia per unit length about the y axis (i.e. an axis through the shear centre) and t is the time and primes and dots denote differentiation with respect to the position y and time t, respectively.

For a free vibration problem, one supposes:

$$\begin{aligned} w(y,t) &= W(y)\sin(\omega t), \\ \psi(y,t) &= \Psi(y)\sin(\omega t), \end{aligned} \tag{3}$$

where $W(y)$ and $\Psi(y)$ are the amplitudes of the sinusoidally varying vertical displacement and torsional rotation, respectively.

Substituting Eq. (3) into Eqs. (1) and (2) gives

$$H_f W'''' - P w'' - m\omega^2 W + (P x_\alpha \Psi'' + m x_\alpha \omega^2 \Psi) = 0, \tag{4}$$

$$(H_t + P(I_\alpha/m))\Psi'' + I_\alpha \omega^2 \Psi - (P x_\alpha W'' + m x_\alpha \omega^2 W) = 0. \tag{5}$$

The integral form associated with Eqs. (1) and (2) can be written as

$$\int_0^L \delta W \{H_f W'''' - P w'' - m\omega^2 W + (P x_\alpha \Psi'' + m x_\alpha \omega^2 \Psi)\}\,\mathrm{d}y = 0, \tag{6}$$

$$\int_0^L \delta \Psi \{(H_t + P(I_\alpha/m))\Psi'' + I_\alpha \omega^2 \Psi - (P x_\alpha W'' + m x_\alpha \omega^2 W)\}\,\mathrm{d}y = 0. \tag{7}$$

Here, W and Ψ are the solution functions and δW and $\delta \Psi$ are test functions. Then, applying an appropriate number of integrations by parts allows us to diminish the derivatives order and the Galerkin type weak form associated with Eqs. (6) and (7) is obtained as

$$\begin{aligned} \mathscr{W}_f = &\int_0^L \left\{H_f \delta W'' W'' + P\delta W' W' - (m\omega^2) \ * \ \delta W W - (P x_\alpha)\delta W' \Psi + (m x_\alpha \omega^2)\delta W \Psi\right\}\mathrm{d}y \\ &+ \left[H_f(\delta W W''' - \delta W' W'') - P\delta W(W' - x_\alpha \Psi')\right]_0^L, \end{aligned} \tag{8}$$

$$\begin{aligned} \mathscr{W}_t = &\int_0^L \{-(H_t + P(I_\alpha/m))\delta\Psi'\Psi' + (I_\alpha\omega^2) \ * \ \delta\Psi\Psi + (P x_\alpha)\delta\Psi' W - (m x_\alpha \omega^2) \ * \ \delta\Psi W\}\,\mathrm{d}y \\ &+ \left[\delta\Psi H_t \Psi' + P\delta\Psi((I_\alpha/m)\Psi' - x_\alpha W')\right]_0^L, \end{aligned} \tag{9}$$

where both solution and test functions are defined in the same approximation space. For clamped–free boundary conditions, for example, it is assumed that

$$\delta W = \delta W' = \delta \Psi = 0 \quad \text{at } y = 0,$$

and force terms are zero at $y = L$. Consequently, the boundary terms in the above expressions will disappear. However, it can be verified that also for any other boundary conditions, similar results can be obtained, when the proper constraints are applied regarding test functions.

Expressions (8) and (9) also satisfy the principle of virtual work (PVW):

$$\mathscr{W} = \mathscr{W}_{INT} - \mathscr{W}_{EXT} = 0, \tag{10}$$

where, for the free vibration analysis,

$$\mathscr{W}_{EXT} = 0,$$

and therefore,

$$\mathscr{W}_{\mathrm{INT}} = \mathscr{W}_{\mathrm{f}} + \mathscr{W}_{\mathrm{t}}.$$

If the domain is discretized by a number of 2-node beam elements [19], we have (Fig. 3)

$$\mathscr{W} = \mathscr{W}_{\mathrm{INT}} = \sum_{k=1}^{\mathrm{NE}} \mathscr{W}^k = 0, \tag{11}$$

where

$$\mathscr{W}^k = \mathscr{W}^k_{\mathrm{f}} + \mathscr{W}^k_{\mathrm{t}}, \tag{12}$$

and

$$\mathscr{W}^k_{\mathrm{f}} = \int_{y_j}^{y_{j+1}} \left\{ H_{\mathrm{f}} \delta W'' W'' + P \delta W' W' - \left(m\omega^2\right) \ * \ \delta W W - (P x_\alpha) \delta W' \Psi' + \left(m x_\alpha \omega^2\right) \delta W \Psi \right\} \mathrm{d}y, \tag{13}$$

$$\mathscr{W}^k_{\mathrm{t}} = \int_{y_j}^{y_{j+1}} \left\{ -(H_{\mathrm{t}} + P(I_\alpha/m)) \delta \Psi' \Psi' + \left(I_\alpha \omega^2\right) \ * \ \delta \Psi \Psi + (P x_\alpha) \delta \Psi' W' - \left(m x_\alpha \omega^2\right) \delta \Psi W \right\} \mathrm{d}y. \tag{14}$$

Each element is defined by nodes j, $j+1$ with corresponding coordinates.

The components of $\mathscr{W}^k$ may also be written in an equivalent form obtained after integration by parts on each element:

$$\begin{aligned} \mathscr{W}^k_{\mathrm{f}} = & \int_{y_j}^{y_{j+1}} W \{ (H_{\mathrm{f}}) \delta W'''' - (P) \delta W'' - (m\omega^2) \delta W \} \, \mathrm{d}y \\ & + [H_{\mathrm{f}} (\delta W'' W' - \delta W''' W) + (P) \delta W' W]_{y_j}^{y_{j+1}} + \int_{y_j}^{y_{j+1}} (-P x_\alpha) \delta W' \Psi' + (m x_\alpha \omega^2) \delta W \Psi \, \mathrm{d}y, \end{aligned} \tag{15}$$

$$\begin{aligned} \mathscr{W}^k_{\mathrm{t}} = & \int_{y_j}^{y_{j+1}} -\Psi \{ (H_{\mathrm{t}} + P(I_\alpha/m) \delta \Psi'' + (I_\alpha \omega^2) \delta \Psi \} \, \mathrm{d}y \\ & + [(H_{\mathrm{t}} + P(I_\alpha/m)) \delta \Psi' \Psi]_{y_j}^{y_{j+1}} + \int_{y_j}^{y_{j+1}} ((-P x_\alpha) \delta \Psi' W' + (m x_\alpha \omega^2) \delta \Psi) W \, \mathrm{d}y. \end{aligned} \tag{16}$$

The admissibility condition for the finite element (FE) approximation is controlled by Eqs. (8) and (9). The approximation for W, δW is of C^1-type, assuring continuity of W and $W_{,x}$ at each node, and the approximation for Ψ, $\delta \Psi$ is of C^0-type. Eqs. (15) and (16) simply present another way of evaluating Eqs. (8) and (9) at the element level.

2.1. The classical finite element method

The classical FE model is found by using the Hermite type polynomial approximation such as

$$W(x) = N_1(x) W_1 + N_2(x) W_1' + N_3(x) W_2 + N_4(x) W_2', \tag{17}$$

where W_1 and W_2 are nodal values at nodes j, $j+1$, corresponding to out-of-plane (flapping) flexural displacements. For torsional displacement $\Psi(x)$, in this case, one uses the linear approximation. Identical approximation is chosen for δW and $\delta \Psi$, respectively. The discretized representation of Eq. (10) is then obtained as

$$\mathscr{W} = \sum_{k=1}^{\mathrm{NE}} \mathscr{W}^k = ([K] - \lambda [M]) \{ w_n \} = 0. \tag{18}$$

This is a classical linear eigenvalue problem which is solved using an inverse iteration procedure, subspace or Lanczos method [20].

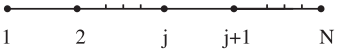

Fig. 3. Domain discretized by a number of 2-node elements.

2.2. The dynamic finite element formulation

In this study, we propose an intermediate approach in which, the classical FEM is combined to the DSM approach, to obtain a better FE model. The approximation space is defined by the frequency dependent hyperbolic functions and the appropriate interpolation functions are obtained with averaged value parameters over each element. The solutions of the uncoupled form of the governing differential equations of motion are utilized, as expansion terms, to find the shape functions. Then, these shape functions, all being frequency dependent, can be used to obtain the corresponding stiffness matrix. In this article, the dynamic finite element (DFE) method is developed and demonstrated for the case of a uniform coupled beam with constant axial loads, where the coefficients H_f, H_t, $m(x)$, P, etc. are constant over the element. Under these circumstances, it would be also possible to write down a general solution for W and Ψ, which leads to an exact DSM [26]. But, it implies complex mathematical procedures and it will be limited to special cases. The advantage of the proposed DFE methodology, comparing with the DSM approach, is that it can be extended to more complex cases as coupled beams with variable geometry and properties. To this end, the interesting features of the DFE methodology presented in the earlier works of the authors, can be exploited (see e.g. Ref. [13]).

To obtain the DFE method formulation, Eqs. (15) and (16) are rearranged in the following equivalent form (see Fig. 4):

$$\mathscr{W}_f^k = \int_0^1 W \underbrace{\left\{\left(\frac{H_f}{l_k^3}\right)\delta W'''' - \left(\frac{P}{l_k}\right)\delta W'' - (ml_k\omega^2)\delta W\right\}}_{*} \mathrm{d}\xi + \left[\left(\frac{H_f}{l_k^3}\right)\{\delta W'' W' - \delta W''' W\} + \left(\frac{P}{l_k}\right)\delta W' W\right]_0^1 + \int_0^1 \left\{\left(\frac{-Px_\alpha}{l_k}\right)\delta W'\Psi' + (ml_k x_\alpha\omega^2)\,\delta W\Psi\right\}\mathrm{d}\xi, \tag{19}$$

$$\mathscr{W}_t^k = \int_0^1 -\Psi \underbrace{\left\{\left(\frac{H_t + P(I_\alpha/m)}{l_k}\right)\delta\Psi'' + (I_\alpha l_k\omega^2)\,\delta\Psi\right\}}_{**} \mathrm{d}\xi + \left[\left(\frac{H_t + P(I_\alpha/m)}{l_k}\right)\delta\Psi'\Psi\right]_0^1 + \int_0^1 \left(\left(\frac{-Px_\alpha}{l_k}\right)\delta\Psi' W' + (ml_k x_\alpha\omega^2)\,\delta\Psi W\right)\mathrm{d}\xi, \tag{20}$$

where $\xi = y/l_k$.

Eqs. (19) and (20) simply present a different way of evaluating Eqs. (13) and (14) at the element level. One can then choose the interpolation functions, which are solutions of the integral terms (*) and (**) in Eqs. (19) and (20) and they respect nodal properties. To this end, using generalized parameters, the non-nodal approximation of the solution function W, Ψ, and the test function $\delta W, \delta\Psi$, can be written as

$$\begin{aligned} \delta W &= \langle P(\xi)\rangle_f * \{\delta a\}, \qquad W = \langle P(\xi)\rangle_f * \{a\}, \\ \delta\Psi &= \langle P(\xi)\rangle_t * \{\delta b\}, \qquad \Psi = \langle P(\xi)\rangle_t * \{b\}, \end{aligned} \tag{21}$$

where the basis functions (i.e., expansion terms) of the approximation are

$$\langle P(\xi)\rangle_f = \left\langle \cos(\alpha\xi)\,\frac{\sin(\alpha\xi)}{\alpha}\,\frac{\cosh(\beta\xi)-\cos(\alpha\xi)}{\alpha^2+\beta^2}\,\frac{\sinh(\beta\xi)-\sin(\alpha\xi)}{\alpha^3+\beta^3}\right\rangle, \tag{22}$$

$$\langle P(\xi)\rangle_t = \langle \cos(\tau\xi)\,\sin(\tau\xi)/\tau\rangle, \tag{23}$$

which are solutions of the integral terms (i.e., (*) and (**)). In addition, they are chosen in such a manner that when α, β and $\tau \to 0$, they lead to classical basis functions of the standard beam element, based on the cubic "Hermite" type interpolation polynomials (for the bending), and the linear ones (for the torsion), respectively. Here,

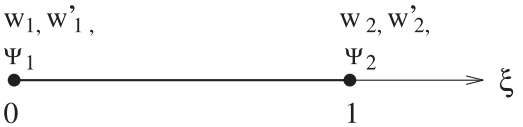

Fig. 4. The 2-node reference element of six degrees of freedom.

$$\begin{aligned}
&\alpha,\beta = \frac{1}{[2\ *\ A]^{1/2}}\{-B \pm [B^2 - 4A *\ C]^{1/2}\}^{1/2},\\
&\tau = \sqrt{I_\alpha \omega^2/H_{\mathrm{t}}},\\
&A = H_{\mathrm{f}}/l_k^3, \quad B = -(P/l_k), \quad C = -(ml_k\omega^2).
\end{aligned} \tag{24}$$

Note that the generalized parameters of the approximation have, in general, no direct physical meaning. Thus, $\langle \delta a\rangle$, $\langle a\rangle$ and $\langle \delta b\rangle$, $\langle b\rangle$ are more conveniently replaced by the nodal variables; $\langle \delta W_1\, \delta W_1'\, \delta W_2\, \delta W_2'\rangle$, $\langle W_1\, W_1'\, W_2\, W_2'\rangle$ and $\langle \delta \Psi_1\, \delta \Psi_2\rangle$, $\langle \Psi_1\, \Psi_2\rangle$, respectively. To this end, one can write (regarding Eq. (21))

$$\{W_n\} = [P_n]_{\mathrm{f}}\ *\{a\}, \qquad \{\delta W_n\} = [P_n]_{\mathrm{f}}\ *\{\delta a\}, \tag{25}$$

$$\{\Psi_n\} = [P_n]_{\mathrm{t}}\ *\{b\}, \qquad \{\delta \Psi_n\} = [P_n]_{\mathrm{t}}\ *\{\delta b\}, \tag{26}$$

where

$$[P_n]_{\mathrm{f}} = \begin{bmatrix} 1 & 0 & 0 & 0 \\ 0 & 1 & 0 & \frac{(\beta-\alpha)}{(\alpha^3+\beta^3)} \\ \cos(\alpha) & \frac{\sin(\alpha)}{\alpha} & \frac{[\cosh(\beta)-\cos(\alpha)]}{(\alpha^2+\beta^2)} & \frac{[\sinh(\beta)-\sin(\alpha)]}{(\alpha^3+\beta^3)} \\ -\alpha\sin(\alpha) & \cos(\alpha) & \frac{[\beta\sinh(\beta)+\alpha\sin(\alpha)]}{(\alpha^2+\beta^2)} & \frac{[\beta\cosh(\beta)-\alpha\cos(\alpha)]}{(\alpha^3+\beta^3)} \end{bmatrix}, \tag{27}$$

$$[P_n]_{\mathrm{t}} = \begin{bmatrix} 1 & 0 \\ \cos(\tau) & \sin(\tau)/\tau \end{bmatrix}. \tag{28}$$

Then, from Eqs. (27), (28) and (21), the $W(\xi)$ and $\Psi(\xi)$ approximations can be rewritten as

$$\begin{aligned}
W(\xi) &= \langle P(\xi)\rangle_{\mathrm{f}}[P_n]_{\mathrm{f}}^{-1}\{W_n\} = \langle N(\xi)\rangle_{\mathrm{f}}\{W_n\},\\
\Psi(\xi) &= \langle P(\xi)\rangle_{\mathrm{t}}[P_n]_{\mathrm{t}}^{-1}\{\Psi_n\} = \langle N(\xi)\rangle_{\mathrm{t}}\{\Psi_n\},
\end{aligned} \tag{29}$$

which represent a nodal approximation of the variables. Similar expressions are also written for the test functions. Eq. (29) can then be rearranged as

$$\begin{Bmatrix} W(\xi) \\ \Psi(\xi) \end{Bmatrix} = [N]\ *\ \{w_n\}; \tag{30}$$

$$\text{where, } \{w_n\} = \langle W_1\, W_1'\, \Psi_1\, W_2\, W_2'\, \Psi_2\rangle^{\mathrm{T}}, \quad [N] = \begin{bmatrix} N_1(\omega)_{\mathrm{f}} & N_2(\omega)_{\mathrm{f}} & 0 & N_3(\omega)_{\mathrm{f}} & N_4(\omega)_{\mathrm{f}} & 0 \\ 0 & 0 & N_1(\omega)_{\mathrm{t}} & 0 & 0 & N_2(\omega)_{\mathrm{t}} \end{bmatrix}. \tag{31}$$

Eq. (31) represents the dynamic shape functions, in matrix form. The analytical expressions of N_i are given in Appendix A. Then, by using Eqs. (19) and (20), the element matrix is obtained as

$$\mathscr{W}^k = \langle \delta w_n\rangle \underbrace{([K_{\mathrm{DS}}]^k_{\mathrm{uncoupl}} + [K_{\mathrm{DS}}]^k_{\mathrm{coupl}})}_{[K_{\mathrm{DS}}]^k}\{w_n\}, \tag{32}$$

where

$$[K_{\mathrm{DS}}]^k_{\mathrm{uncoupl}} = \begin{bmatrix} \underbrace{c_{\mathrm{f}}\{N_{\mathrm{f}}'''\}; c_{\mathrm{f}}\{-N_{\mathrm{f}}''\}; c_{\mathrm{t}}\{-N_{\mathrm{t}}'\}}_{\xi=0}; & \underbrace{c_{\mathrm{f}}\{-N_{\mathrm{f}}'''\}; c_{\mathrm{f}}\{N_{\mathrm{f}}''\}; c_{\mathrm{t}}\{N_{\mathrm{t}}'\}}_{\xi=1} \end{bmatrix}, \tag{33}$$

$$[K_{\mathrm{DS}}]^k_{\mathrm{coupling}} = \begin{bmatrix} 0 & 0 & (K_{\mathrm{C}})_{11} & 0 & 0 & (K_{\mathrm{C}})_{21} \\ & 0 & (K_{\mathrm{C}})_{12} & 0 & 0 & (K_{\mathrm{C}})_{22} \\ & & 0 & (K_{\mathrm{C}})_{13} & (K_{\mathrm{C}})_{14} & 0 \\ & & & 0 & 0 & (K_{\mathrm{C}})_{23} \\ & \text{Sym.} & & & 0 & (K_{\mathrm{C}})_{24} \\ & & & & & 0 \end{bmatrix}, \tag{34}$$

where

$$(K_{\mathrm{C}})_{ij} = \int_0^1 C_p \ * \ N'_{i\mathrm{t}} N'_{j\mathrm{f}} + C_{x_\alpha} \ * \ N_{i\mathrm{t}} N_{j\mathrm{f}} \, \mathrm{d}\xi, \quad \text{for } i = 1,2, \ \ j = 1,2,3,4. \tag{35}$$

and

$$c_{\mathrm{f}} = \frac{H_{\mathrm{f}}}{l_k^3}, \quad c_{\mathrm{t}} = \frac{H_{\mathrm{t}}}{l_k}, \quad C_p = m x_\alpha l_k \omega^2, \quad C_{x_\alpha} = \frac{-P x_\alpha}{l_k}.$$

It can be readily verified from Eqs. (32)–(35) that if the axial force "P" is assumed to be zero, the resultant stiffness matrix is found to be that representing the coupled bending-torsion vibration of uniform beam elements. One can also realize that the second term in Eq. (32), representing the coupling between flexural and torsional vibrations of the beam element, reduces to zero, when $x_\alpha = 0$ ($x_\alpha = 0$ can be substituted in the derived expressions without causing any overflow or underflow). Thus, the stiffness matrix, in this case, reduces to the stiffness matrix representing the uncoupled flexural and torsional vibrations of an axially loaded Euler–Bernoulli beam element [11]. Furthermore, if both of the axial force P and x_α are assumed to be equal zero, the degenerated stiffness matrix of Eq. (32) becomes the stiffness matrix representing the uncoupled flexural and torsional vibrations of an Euler–Bernoulli beam element [17,21]. It can be also verified that when $\omega \to 0$, the functions of Eqs. (22) and (23) become $\langle 1\, x\, x^2\, x^3 \rangle$ and $\langle 1\, x \rangle$, respectively. The former, represents the expansion terms in the formulation of the "Hermite" beam element, in conventional FEM, when flexural degrees of freedom are considered. The latter, corresponds to the expansion terms, in a linear element formulation in conventional FEM, when the torsion of a beam element is studied. In this case, the shape functions of Eq. (30) become the corresponding shape functions actually used in static conventional FEM. Therefore, the DSM of Eq. (32) changes to a static stiffness matrix of a "Hermite" beam element, when the torsion is also included by using a linear approximation [19].

The DFE developed here, covers the coupled bending-torsion vibrations of uniform beams of symmetric cross-section, in the presence of a constant axial load. When designing real blades, the three DOF, namely flap, lag and torsion, have to be usually treated together [9]. However, as mentioned before, the effects of variable centrifugal force, geometrical parameters and mechanical properties, etc., could also be introduced in the formulation by using similar techniques as presented in previous works of the authors [10–15]. We also note that the DFE method can be used for the vibrational analysis of beam assemblages with attached rigid members [22]. Thus, it provides also a basis for analysis of a beam model of helicopter blades with tip mass, balancing masses, etc.

3. Application of the theory

Elementary matrices, $[K_{\mathrm{DS}}]^k$, derived in the previous section, will have to be assembled in the usual way to form the overall DSM $[K_{\mathrm{DS}}]$ of the final structure. The eigenvalue problem resulting from this method, for free vibrations, is then found to be as

$$[K_{\mathrm{DS}}] \ * \ \{W_n\} = \{0\}, \tag{36}$$

which is non-linear. The natural frequencies is then obtained by using Eq. (36) and the well-known Wittrick–Williams algorithm described on several occasions in the literature (e.g. see Refs. [16,17,22,23]). Basically, the algorithm relies on the stiffness matrix of the individual members (DFEs) in the structure and also it requires the knowledge of clamped–clamped frequencies of all such members. The consideration of clamped–clamped frequencies of individual members in a structure is fundamental to the application of the algorithm to ensure that, when finding natural frequencies, none is missed [8]. The procedure is briefly summarized as follows:

Suppose that ω denotes the circular frequency of the beam. Then, it is known that j, the number of eigenvalues passed as ω is increased from zero to ω^*, is given by

$$j = j_0 + s\{K_{\mathrm{DS}}\}, \tag{37}$$

where $[K_{DS}]$ is the overall DSM (which is ω dependent) of the structure, evaluated at $\omega = \omega^*$; $s\{K_{DS}\}$ is the number of negative elements on the leading diagonal of K_{DS}^A, K_{DS}^A is the upper triangular matrix obtained by applying the usual form of Gauss elimination to K_{DS} and j_0 is the number of natural frequencies of the beam still lying between $\omega = 0$ and $\omega = \omega^*$, when the displacement components to which K_{DS} corresponds are all zero (the beam can still have natural frequencies, when all its nodes are clamped, because the presented formulation allows each individual element to have an infinite number of degrees of freedom between nodes). Thus,

$$j_0 = \sum_{m=1}^{EN} j_m \tag{38}$$

where j_m is the number of natural frequencies between $\omega = 0$ and $\omega = \omega^*$ for an element with its ends clamped, whereas the summation extends over all elements.

For the element stiffness matrix developed in this article, the clamped–clamped frequencies of an individual element occurs, when one or more of the components of the matrices of Eqs. (32)–(34) become infinite (i.e. $D_f = 0$ or $D_t = 0$, where D_f and D_t are, respectively, the denominators in flexural and torsional dynamic shape functions, given in expressions (30)).

$D_f = 0$, represents the natural frequencies of flexural vibrations of an axially loaded clamped–clamped uniform beam element. To find j_f (the number of natural frequencies between $\omega = 0$ and $\omega = \omega^*$), one can use an indirect method [24] by considering

$$j_f = j_c - s\{B\}, \tag{39}$$

where j_c is the number of natural frequencies of the simply supported beam exceeded by ω^*,

$$j_c = \text{the highest integer} < \frac{\alpha}{\pi} \tag{40}$$

and $s\{B\}$ is the number of negative elements on the leading diagonal of B^A, B^A is the upper triangular matrix obtained by applying the usual form of Gauss elimination to B.

$D_t = 0$, represents the natural frequencies of torsional vibrations of a uniform clamped–clamped beam, and the number of these natural frequencies exceeded by any trial ω is given by

$$j_t = \text{the highest integer} < \frac{\tau}{\pi}. \tag{41}$$

Hence

$$j_m = j_f + j_t \tag{42}$$

and j_0 follows from Eq. (38).

Thus, with the knowledge of Eqs. (37)–(42), it is possible to converge on any required natural frequency. Then, the mode shapes are calculated using Eq. (36). This procedure is implemented in an existing conventional FE program called RE-FLEX [25] to obtain the results given in Section 4.

4. Numerical tests

Numerical checks are performed to confirm the predictability and accuracy of the theory. The coupled bending-torsional natural frequencies for a variety of open and closed section unloaded beams were studied by substituting $P = 0$ in the data and a very good agreement was found with published results [15,26–28]. Further, it was also verified that assuming both $P = 0$ and $x_\alpha = 0$, the exact natural frequencies of free bending and torsional vibrations of beams can be obtained [17].

In what follows, an illustrative example of a bending-torsion coupled beam with monosymmetric semi-circular cross-section, presented by Friberg [18] is investigated.

First, the clamped–free natural frequencies of this example are studied, when the axial force P is simply assumed to be zero. Then, the effect of a constant axial force on the natural frequencies and mode shapes, is studied. The following cross-sectional properties were used in the calculation (see Fig. 5 for details) [18]:

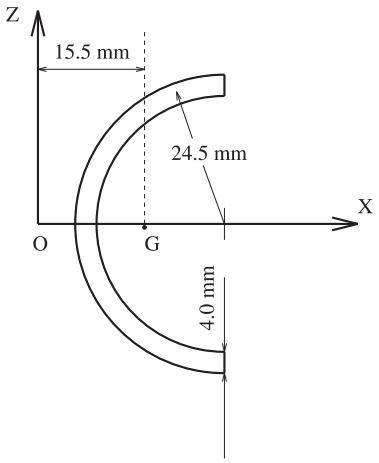

Fig. 5. Cross-sectional details of the analyzed bending-torsional coupled beam.

(i) radius $(r) = 24.5$ mm,
(ii) thickness $(t) = 4.0$ mm,
(iii) the distance between the shear centre and centroid $(x_\alpha) = 15.5$ mm,
(iv) mass per unit length $(m) = 0.835$ kg/m,
(v) polar mass moment of inertia per unit length $(I_\alpha) = 501 \times 10^{-6}$ kg m,
(vi) cross-sectional area $(A) = 308 \times 10^{-6}$ m^2,
(vii) second moment of inertia about x axis $(I_{XX}) = 92.6 \times 10^{-9}$ m^4,
(xiii) $E = 68.9$ GPa,
(ix) $G = 26.5$ GPa,
(x) length of the beam (L) was assumed to be 0.82 m.

The natural frequencies obtained by the DFE method, together with the exact results and those found by the classical FEM are given in Table 1. The exact results are found by employing the DSM presented in Ref. [26] (which is the same as the DSM presented in Ref. [8] when $P = 0$). The classical FEMs results are calculated from the FE presented in Ref. [1]. The static stiffness and mass matrices, in that case, were found using a cubic "Hermite" type and linear approximations for flexural and torsional displacements, respectively. They were calculated, when the beam was discretized by 200 elements of equal length and an 'inverse iteration' solution method was used. In this case, it was observed that the FEM leads to the natural frequencies which are slightly different from the exact values (the error was about 0.2%). This fact can be attributed to the iterative nature of the adopted solution method. However, similar tests for the DFE showed excellent convergencies (the corresponding results of Table 1 are found, when only five DFEs are used).

Fig. 6 represents the DFE convergency tests corresponding to the first three clamped-free natural frequencies of the beam. As can be seen for the first natural frequency, the error is found to be approximately zero ($\varepsilon \leqslant 0.1\%$), even when

Table 1
Bending-torsional natural frequencies of coupled beam based on the present theory[a], exact DSM method[b] and classical FE[c] ($P = 0$)

i	Frequency f_i (Hz)				
	DFE[a]	Exact DSM[b]	$\lvert\text{Error}_{1-2}\rvert$ (%)	Classical FEM[c]	$\lvert\text{Error}_{2-3}\rvert$ (%)
1	62.5	62.5	0.0	62.6	0.2
2	130.5	130.0	0.4	130.2	0.2
3	261.8	261.0	0.3	261.2	0.1

[a] The results found by using only five DFEs.
[b] The results obtained using the exact DSM method [26,8].
[c] The results obtained using 200 classical FEs [1].

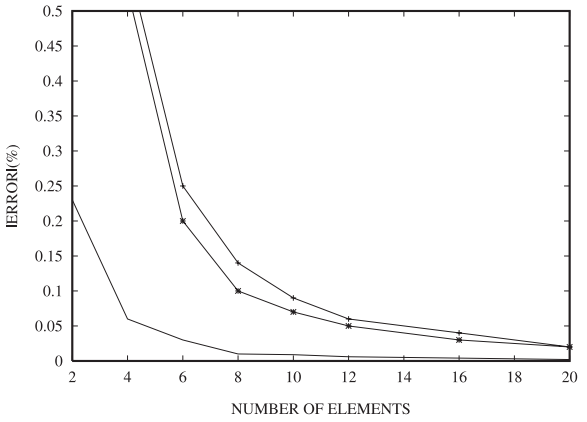

Fig. 6. Convergency test for the first three natural frequencies of the clamped–free bending-torsion coupled beam (with $P = 0$). —, ω_1; — $*$ —, ω_2; — $+$ —, ω_3.

only four elements are used. For the second and third natural frequencies, the results are converging with approximately 0.1% percent error, when eight elements are used.

In the second part of this example, the effect of a compressive axial force is studied. The first three coupled bending-torsional natural frequencies (ω_i) of the beam, with cantilever end conditions and the axial load $P = -1790$ N, are calculated using the DFE method. The comparison was made between these results and those available in the literature [18,8]. The natural frequencies, obtained using only six DFEs, are given in Table 2 alongside the published results obtained using the exact DSM method [8] and Vlasov's theory [18]. The maximum disagreement between the calculated results, obtained using six DFEs, and the exact results found from DSM [8] is about 0.2%. When comparing these results, obtained using six DFEs, to those obtained from Vlasov's theory [18], the maximum disagreement is found to be about 6%. The difference can be attributed to the fact that no allowance has been made in the present theory for stiffness associated with warping of the beam cross-section. However, the errors incurred are expected to be significantly less for closed and solid sections as applicable to helicopter and turbine blades [6], for which the warping term plays a relatively minor role.

It can be seen from Tables 1 and 2 that the frequency of the beam is reduced because of compressive axial loads. A similar test was repeated for a tensile axial load ($P = +1790$ N) and the first three natural frequencies were found as $f_1 = 64.7$ Hz, $f_2 = 132.3$ Hz and $f_3 = 264.9$ Hz, respectively. As can be observed, the frequency increases with tensile loads, although not as fast as it reduces with compressive loads. These results are in accord with an earlier work of Banerjee and Fisher [8].

The mode shapes corresponding to the first three clamped–free natural frequencies, for $P = 0$ N, $P = -1790$ N and $P = +1790$ N, are given in Fig. 7. As can be seen, the axial force has not a pronounce effect on the torsional displacements. Regarding the flexural displacement, the influence of axial forces on the first mode is visible, whereas the other modes are much less affected (i.e., A compressive axial force renders the beam less stiff, whereas a tensile one has a stiffening effect). The natural frequencies are well separated, but the generated modes show substantial coupling between flexural and torsional rotations.

Table 2
Natural frequencies of axially loaded bending-torsion coupled beam using the DFE theory[a], exact DSM method[b] and Vlasov theory[c]

i	Frequency f_i (Hz)				
	DFE[a]	Exact DSM[b]	$\lvert Error_{1-2} \rvert$ (%)	Vlasov theory[c]	$\lvert Error_{1-3} \rvert$ (%)
1	60.11	60.23	0.20	61.28	1.91
2	128.6	128.4	0.16	136.0	5.44
3	258.4	258.0	0.16	274.9	6.00

[a] The presented results are found by using only six DFEs.
[b] The published results obtained using the exact DSM method [8].
[c] The published results obtained using Vlasov's theory [18].

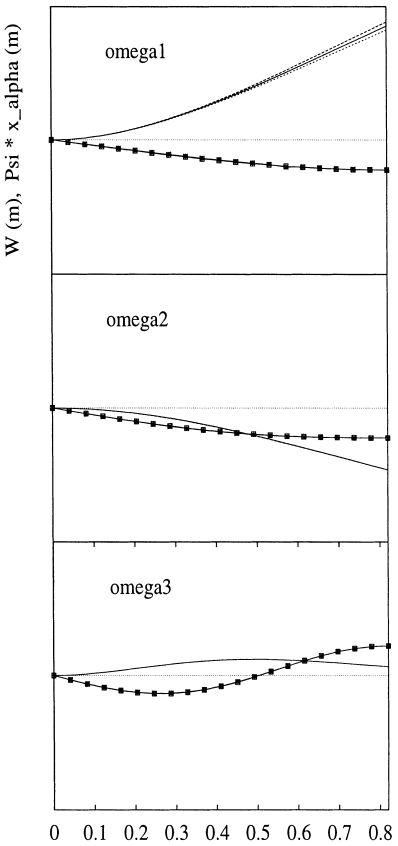

Fig. 7. The coupled bending-torsional natural frequencies and modes of semi-circular beam: (—), flexural displacement (W) for $P = 0$; (- - -), flexural displacement (W) for $P < 0$; (— — —), flexural displacement (W) for $P > 0$; (—■—), torsional displacement ($\Psi \cdot x_\alpha$) for $P = 0$; (— – ×—–), torsional displacement for $P < 0$; (. . .), torsional displacement for $P > 0$.

5. Conclusion

A DFE for the natural frequencies and mode calculation of coupled bending-torsion vibration of axially loaded beams is presented. Based on the closed form solutions of the Euler–Bernoulli and St. Venant beam theories, respectively, the trigonometric shape functions corresponding to the uncoupled bending and torsional vibrations were found. The symbolic computing package MATHEMATICA was used in deriving and simplifying these expressions. Then, they were used to derive the DFE stiffness matrix. A root counting technique for isolating the clamped–clamped bending natural frequencies of the beam was also given to enable an established algorithm to be used to guarantee convergence on all required natural frequencies of free vibration of such beams. The results obtained from the present theory were found to be in good agreement with the published results. The DFE approach can also be advantageously extended to cover more complex problems such as coupled biaxial bending-torsion vibration of rotating (centrifugally stiffened) beams with uniform or non-uniform geometries.

Acknowledgements

Special thanks to Prof. G. Dhatt, from l'INSA de Rouen (France), for valuable comments and scientific discussions. The first author wishes to acknowledge the scholarship awarded by the Ministry of Culture and Higher Education of Iran, which made this work possible. The authors are also grateful to the Natural Sciences and Engineering Research Council of Canada, which also supported this research.

Appendix A. Flexural and torsional dynamic shape functions

$$N_1(\omega)_f OO = \frac{(\alpha\beta)}{D_f} * \{ -\cos(\alpha\xi) + \cos(\alpha(1-\xi)) * \cosh(\beta) + \cos(\alpha) * \cosh(\beta(1-\xi)) - \cosh(\beta\xi) - \frac{\beta}{\alpha} * \sin(\alpha(1-\xi)) * \sinh(\beta) + \frac{\alpha}{\beta} * \sin(\alpha) * \sinh(\beta(1-\xi))\}, \tag{A.1}$$

$$N_2(\omega)_f = \frac{1}{D_f} * \{\beta * [\cosh(\beta(1-\xi)) * \sin(\alpha) - \cosh(\beta) * \sin(\alpha(1-\xi)) - \sin(\alpha\xi)] + \alpha * [\cos(\alpha(1-\xi)) * \sinh(\beta) - \cos(\alpha) * \sinh(\beta(1-\xi)) - \sinh(\beta\xi)]\}, \tag{A.2}$$

$$N_3(\omega)_f = \frac{(\alpha\beta)}{D_f} * \left\{ -\cos(\alpha(1-\xi)) + \cos(\alpha\xi) * \cosh(\beta) - \cosh(\beta(1-\xi)) + \cos(\alpha) * \cosh(\beta\xi) - \frac{\beta}{\alpha} * \sin(\alpha\xi) * \sinh(\beta) + \frac{\alpha}{\beta} * \sin(\alpha) * \sinh(\beta\xi) \right\}, \tag{A.3}$$

$$N_4(\omega)_f = \frac{1}{D_f} * \{\beta * [-\cosh(\beta\xi) * \sin(\alpha) + \sin(\alpha(1-\xi)) + \cosh(\beta) * \sin(\alpha\xi)] - \alpha * [\cos(\alpha\xi) * \sinh(\beta) + \sinh(\beta(1-\xi)) + \cos(\alpha) * \sinh(\beta\xi)]\}. \tag{A.4}$$

The torsional dynamic shape functions are found to be as

$$N_1(\omega)_t = \cos(\tau\xi) - \cos(\tau) * \frac{\sin(\tau\xi)}{D_t} \tag{A.5}$$

$$N_2(\omega)_t = \frac{\sin(\tau\xi)}{D_t}, \tag{A.6}$$

where

$$D_f = (\alpha\beta) * \left\{ -2 * (1 - \cos(\alpha) * \cosh(\beta)) + \left(\frac{\alpha^2 - \beta^2}{\alpha\beta} \right) * \sin(\alpha) * \sinh(\beta) \right\}, \tag{A.7}$$

$$D_t = \sin(\tau). \tag{A.8}$$

References

[1] Hallauer WL, Liu RYL. Beam bending-torsion dynamic stiffness method for calculation of exact vibration modes. J Sound Vibr 1982;85:105–13.
[2] Banerjee JR. Flutter characteristics of high aspect ratio tailless aircraft. J Aircraft 1984;21:733–6.
[3] Banerjee JR. Flutter modes of high aspect ratio tailless aircraft. J Aircraft 1988;25:473–6.
[4] Friedmann PP, Straub F. Application of the finite element method to rotary-wing aeroelasticity. J Am Helicopter Soc 1980;25: 36–44.
[5] Houbolt JC, Brooks GW. Differential equations of motion for combined flap-wise bending, chordwise bending, and torsion of twisted nonuniform rotor blades, NACA Report No. 1346, 1958.
[6] Subrahmanyam KB, Kulkarni SV, Rao JS. Application of the Reissner method to derive the coupled bending-torsion equations of dynamic motion of rotating pretwisted cantilever blading with allowance for shear deflection, rotary inertia, warping and thermal effects. J Sound Vibr 1982;84(2):223–40.
[7] Dżygadlo Z, Sobieraj W. Natural flexural-torsional vibration analysis of helicopter rotor blades by the finite element method. J Tech Phys 1977;18(4):443–54.
[8] Banerjee JR, Fisher SA. Coupled bending-torsional dynamic stiffness matrix for axially loaded beam elements. Int J Numer Meth Engng 1992;33:739–51.
[9] Newman S. The foundations of helicopter flight. New York: Halsted Press, an imprint of Wiley, 1994.
[10] Hashemi SM, Richard MJ, Dhatt G. A Bernoulli–Euler stiffness matrix approach for vibrational analysis of linearly tapered beams. In: Proceedings of the Acoustics Week in Canada. Calgary, Alta., Canada, 1996. p. 87.

[11] Hashemi SM, Richard MJ, Dhatt G. A dynamic finite element (DFE) formulation for free vibration analysis of centrifugally stiffened uniform beams. In: Proceedings of the16th Canadian Congress of Applied Mechanics (CANCAM 1997). Québec, Que., Canada, 1997. p. 443–4.
[12] Hashemi SM, Richard MJ, Dhatt G. A Bernoulli–Euler stiffness matrix approach for vibrational analysis of spinning linearly tapered beams. ASME paper no. 97-GT-500, 42nd ASME Gas Turbine and Aeroengine Congress, Orlando, FL.
[13] Hashemi SM, Richard MJ, Dhatt G. A new dynamic finite element (DFE) formulation for lateral free vibrations of Euler–Bernoulli spinning beams using trigonometric shape functions. J Sound Vibr 1999;220(4):601–29.
[14] Hashemi SM, Richard MJ. On the coupled bending-torsional natural frequencies and modes of beams; a frequency dependent dynamic finite element (DFE). In: Proceedings of the Canadian Society for Mechanical Engineering (CSME) Forum. Toronto, Ont., Canada, 1998. p. 468–575.
[15] Hashemi SM, Richard MJ, Dhatt G. A dynamic finite element (DFE) approach for coupled bending-torsional vibrations of beams. In: Proceedings of the 39th AIAA/ASME/ASCE/AHS/ASC Structures, Structural Dynamics, and Materials Conference, paper no. AIAA-98-2020. Long Beach, CA, 1998. p. 2614–24.
[16] Williams FW, Wittrick WH. An automatic computational procedure for calculating natural frequencies of skeletal structures. Int J Mech Sci 1970;12:781–91.
[17] Wittrick WH, Williams FW. A general algorithm for computing natural frequencies of elastic structures. Quart J Mech Appl Math 1971;24:263–84.
[18] Friberg PO. Beam element matrices derived from Vlasov's theory of open thin-walled elastic beams. Int J Numer Meth Engng 1985;21:1205–28.
[19] Dhatt G, Touzot G. Paris et Les presses de L'Université Laval. In: Maloine SA, editor. Une présentation de la méthode des éléments finis. Québec, Que., Canada, 1981. p. 100–3. [in French].
[20] Bathe KJ. Finite element procedure in engineering analysis. Englewood Cliffs, NJ: Prentice-Hall, 1982.
[21] Wittrick WH, Williams FW. On the free vibration analysis of spinning structures by using discrete or distributed mass models. J Sound Vibr 1982;82(1):1–15.
[22] Åkesson BÅ. PFVIBAT – a computer program for plane frame vibration analysis by an exact method. Int J Numer Meth Engng 1976;10:1221–31.
[23] Swannell P. The automatic computation of the natural frequencies of structural frames using an exact matrix technique. Theory and practice in finite element structural analysis. Tokyo: University of Tokyo Press, 1973. p. 289–304.
[24] Howson WP, Williams FW. Natural frequencies of frames with axially loaded Timoshenko members. J Sound Vibr 1973;26(4):503–15.
[25] Batoz JL, Dhatt YG. REF_LEX – Recherche et Enseignement en modélisation des structures FLEXible, Division MNM/Département GM, Université de technologie de Compiegne, France.
[26] Banerjee JR. Coupled bending-torsional dynamic stiffness matrix for beam elements. Int J Numer Meth Engng 1989;28:1283–98.
[27] Goland M. Flutter of a uniform cantilever wing. J Appl Mech 1945;12:A197–208.
[28] Eslimi-Isfahani SHR, Banerjee JR, Sobey AJ. Response of a bending-torsion coupled beam to deterministic and random loads. J Sound Vibr 1996;195(2):267–83.